

## Paleoceanographic reconstruction of the western equatorial Atlantic during the last 40 kyr



Thiago P. Santos<sup>a</sup>, Andre L. Belem<sup>a</sup>, Catia F. Barbosa<sup>a</sup>, Trond Dokken<sup>b</sup>, Ana Luiza S. Albuquerque<sup>a,\*</sup>

<sup>a</sup> Departamento de Geoquímica, Universidade Federal Fluminense, Outeiro de São João Batista, s/no., Niterói, Rio de Janeiro CEP: 24020-141, Brazil

<sup>b</sup> Bjerknes Centre for Climate Research, Allégaten 55, NO-5007 Bergen, Norway

### ARTICLE INFO

#### Article history:

Received 11 June 2013

Received in revised form 21 December 2013

Accepted 1 January 2014

Available online 14 January 2014

#### Keywords:

Oxygen stable isotopes

Sea surface temperature

Sea surface salinity

Planktonic foraminiferal assemblage

Atlantic Meridional Overturning Circulation

### ABSTRACT

The North Brazil Current in the western equatorial Atlantic is the main route for poleward heat transfer and therefore is a key component of the climate system. To understand the parameters that influence this region, we present a paleoceanographic reconstruction of the last 40 kyr based on study of sediment core MC 10/3. This reconstruction is based on: i) the oxygen isotope composition of the planktonic foraminifer *Globigerinoides ruber* (white); ii) census counts of the planktonic foraminifera assemblage to estimate sea surface temperature (SST) via the Modern Analogue Technique ( $SST_{MAT}$ ) and to deduce characteristics of the water column; and iii) values of  $\delta^{18}O_{IVC-SW}$  (a proxy for sea surface salinity (SSS)). The oxygen isotope composition of *G. ruber* showed a strong shift of greater than 1‰ after 21 cal kyr BP. Such a change can be attributed mainly to a salinity reduction of two units, as well as a slight SST increase ( $\sim 1^\circ\text{C}$ ), between 21 and 17.5 kyr BP. This change may be related to a southward displacement of the Intertropical Convergence Zone (ITCZ) and its belt of convective activity, which would have increased precipitation over the region and diminished surface salinity. The structure of the planktonic foraminiferal assemblage also indicates such conditions. The productive/thermocline-dwelling *Globigerinita glutinata* showed higher abundance prior to 21 cal kyr BP. Other productive/deep-dwellers, i.e., *Neogloboquadrina dutertrei*, *Globorotalia truncatulinoides* (left- and right-coiling) and *Globorotalia inflata*, were slightly more abundant prior to 21 cal kyr BP and became less frequent with the development of low-salinity surface water that created more stratified and oligotrophic conditions in the water column. However, the warm/oligotrophic surface-dwellers (*G. ruber*, *Globigerinoides sacculifer* and *Globigerinella siphonifera*) became more abundant after 21 cal kyr BP. The species *Globorotalia menardii* was nearly absent during the Last Glacial Maximum (LGM), and its growth in abundance, mainly after 17.5 cal kyr BP, may indicate the resumption of the Agulhas leakage, which would have reached the study area via the South Equatorial Current (SEC). The return of high salinity values synchronous with the *G. menardii* increase also denotes the influence of Agulhas leakage into the western equatorial Atlantic.

© 2014 Elsevier B.V. All rights reserved.

### 1. Introduction

The equatorial Atlantic Ocean is an important driving force for climatic change due to its impact on the density of high-latitude surface waters (Zickfeld et al., 2007). The western portion of the equatorial Atlantic comprises part of the Atlantic Meridional Overturning Circulation (AMOC), which is one of the most important components of the Earth's climate, particularly because it controls the amount of heat transported northward along the meridional Atlantic (Guihou et al., 2011).

Studies regarding AMOC sensitivity, e.g., Goelzer et al., 2006, show that a freshwater influence from the equatorial Atlantic leads to a weakening of the AMOC. As a result, the surface air temperatures over the North Atlantic cool, and temperatures over the South Atlantic warm (Barker et al., 2009). This conceptual model, known as thermal

bipolar seesaw, implies that during the last deglaciation, the magnitude of heat release from the Southern Ocean was out of phase with that in the northern Atlantic (Broecker, 1998).

Sea surface temperature (SST) reconstructions based on planktonic foraminiferal assemblages showed that the glacial cooling in the central North Atlantic reached a maximum of  $12^\circ\text{C}$  (Pflaumann et al., 2003). In contrast, SST reconstructions for the western subtropical gyre of the South Atlantic indicated a smaller cooling of approximately  $1\text{--}2^\circ\text{C}$  (Niebler et al., 2003). Such a temperature gradient between the North and South Atlantic Ocean shifted the Intertropical Convergence Zone (ITCZ) to its southernmost position, especially during the boreal winter, producing relatively humid conditions in northeastern Brazil and dry conditions in northern South America (Arz et al., 1998; Peterson and Haug, 2006).

In addition, strong precipitation in the ITCZ also led to a region of low sea surface salinity (SSS) around  $5^\circ\text{N}$ , which could have had an important role in ocean circulation due to buoyancy and stratification of the water column (Da-Allada et al., 2013). Based on this finding, we

\* Corresponding author. Tel.: +55 21 2629 2197.

E-mail address: [ana\\_albuquerque@id.uff.br](mailto:ana_albuquerque@id.uff.br) (A.L.S. Albuquerque).

present a SST and SSS reconstruction that combines planktonic foraminifera census counts and oxygen stable isotopes from the western equatorial Atlantic for the last 40,000 yr.

## 2. Oceanographic features of the multicore MC 10/3 area

The multicore GS07-150 MC-B 10/3 (hereafter abbreviated as MC 10/3) was collected during the G. O. Sars cruise from a water depth of 939 m at coordinates 4°49.376'S and 34°52.956'W, near the northern Brazilian margin (Fig. 1). The study area is influenced by the North Brazil Current (NBC), which is generated by the bifurcation of the South Equatorial Current (SEC) at approximately 10°S (Schott et al., 1995).

The flow of the NBC and its large anticyclonic rings is the main pathway in the western equatorial Atlantic for the transport of upper-ocean waters northwest across the equator (Goni and Johns, 2001). This inter-hemispheric heat transport requires a northward cross-equatorial mass flux in the upper layers that is compensated by the southward transport of the North Atlantic Deep Waters (NADW) in the lower layers (Haarsma et al., 2011).

However, the northwestern heat transport performed by the NBC exhibits seasonal circulation variability. Between July and February, the surface layer of the NBC separates from the coast at approximately 8°N and mixes into the North Equatorial Countercurrent (NECC) in a process known as NBC retroflexion (NBCR) (Fonseca et al., 2004). From March through June, the majority of the NBC continues to the northwest along the continental slope off the coast of South America, eventually entering the Caribbean Sea and feeding the Gulf Stream (Johns et al., 1998; Lux et al., 2001).

The study area is characterized by two modes of ocean–atmosphere variability that significantly affect the regional climates of the Americas and Africa (Servain et al., 1998). The first mode is similar to the El-Niño Southern Oscillation and is manifested as warm and cold phases focused near the equator (Chang et al., 1997). The second mode is characterized by a north–south inter-hemispheric SST gradient, i.e., the Atlantic dipole (Chang et al., 1997).

The seasonal cycle of the surface currents reflects the response to the seasonally variable wind field and the migration of the ITCZ (Stramma and Schott, 1999). The cross-equatorial SST gradient causes a meridional pressure gradient across the equatorial Atlantic. This surface pressure drives cross-equatorial meridional winds that are thought to affect the position of the ITCZ (Chiang et al., 2003). When the ITCZ and the associated changes in the wind stress curl are in their northernmost positions (during boreal summer and fall), the maximum northward transport by the NBC occurs between 0° and 5°N (Johns et al., 1998).

The Agulhas Leakage represents an additional major influence on the study area and global climate. The warm, saline waters from the Indian Ocean help drive upper Atlantic circulation towards the subpolar northern Atlantic. Recent modeling work (e.g., Biastoch et al., 2008; Marino et al., 2013) has suggested that dynamic signals originating in the Agulhas Leakage region contribute to decadal- to millennial-time scale AMOC variability on the same order of magnitude as the often invoked northern source. Over longer periods, Agulhas Leakage variability is associated with the large-scale wind field, in particular with the position of the maximum Southern Hemisphere westerly winds (Beal et al., 2011).

## 3. Material and methods

The total length of multicore MC 10/3 was 40 cm, and the core was sliced every 0.5 cm by extrusion. The age model was based on five carbonate (*Globigerinoides ruber*) AMS radiocarbon ages analyzed at the NSF-Arizona AMS Facility (Table 1). The ages were calibrated using the Calib 6.0 software (Stuiver et al., 1998) with a standard marine correction of 400 yr and a regional reservoir effect of  $\Delta R = 8 \pm 17$  yr (Angulo et al., 2005). Calibrated ages between  $2\sigma$  intervals were interpolated by using linear regression (Fig. 2). The highest rate of sedimentation, between 25.5 and 15 cm (around 30 cal kyr BP), may be the result of rapid sea-level fall in the early portion of the last glacial.

Oxygen isotope analyses ( $\delta^{18}O_c$ ) were performed on the tests of 15 specimens of *G. ruber* (white) from the 250–300  $\mu$ m size fraction. The analyses were conducted by using a Finnigan MAT 252 spectrometer

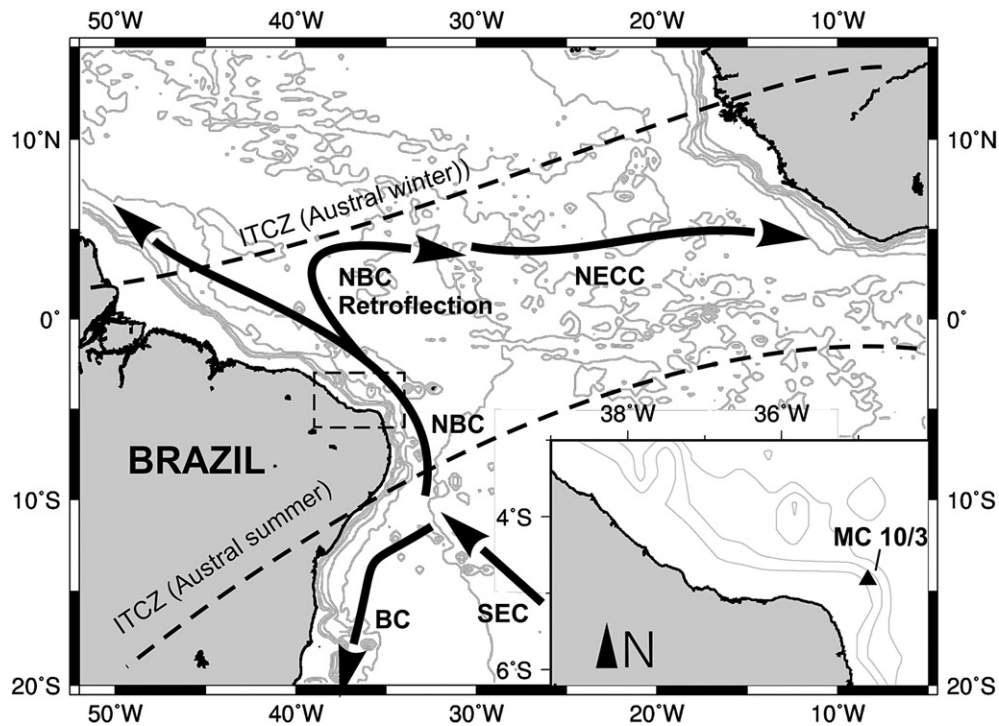


Fig. 1. The study area with a schematic illustration of the mean surface circulation along the Northeast Brazilian Margin. SEC: South Equatorial Current. BC: Brazil Current. NBC: North Brazil Current (and its retroflexion). NECC: North Equatorial Countercurrent. The dashed lines represent the seasonal position of the ITCZ – Intertropical Convergence Zone.

**Table 1**AMS radiocarbon ages of the selected samples. The calibrated ages were calculated using the SW Atlantic reservoir effect ( $\Delta R = 8 \pm 17$ ), according to Angulo et al. (2005).

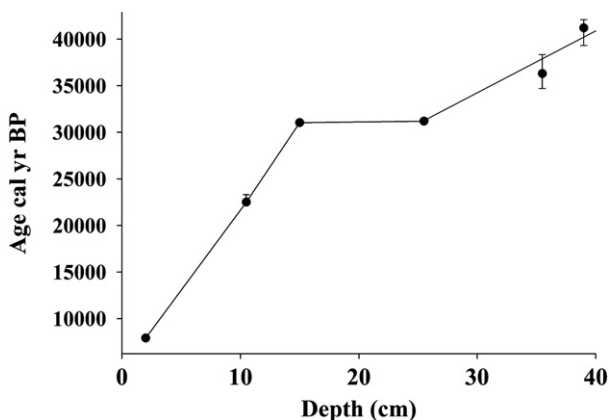
Lab code	Sample (cm)	Age $^{14}\text{C}$ BP	Age error	cal year BP	Lower (cal yr BP)	Upper (cal yr BP)
AA89725	2	7429	53	7910	7755	7995
AA90162	10.5	19,320	230	22,500	22,048	23,363
AA89726	15	26,790	230	31,040	30,590	31,277
AA90164	25.5	27,105	261	31,190	30,848	31,482
AA90166	35.5	31,961	1045	36,300	34,120	34,362
AA89727	39	36,450	750	41,200	39,312	42,252

at the Stable Isotope Laboratory of the University of California, Davis, USA, with a precision of  $\pm 0.04\%$ . The samples were reacted in 105%  $\text{H}_3\text{PO}_4$  at 90 °C using a Gilson Multicarb Autosampler. The data were calculated relative to VPDB by using the NBS-19 calcite standard.

Planktonic foraminifera were analyzed from 1  $\text{cm}^3$  of sediment that was first washed through a 150  $\mu\text{m}$  mesh sieve. The samples were then dried at temperatures below 50 °C for 24 h. The 150  $\mu\text{m}$  size fraction was split by using a microsplitter until a minimum of 300 foraminifera were selected. Tests were identified by using stereomicroscopy, and identification was performed according to previous studies (Parker, 1962; Bé, 1977; Kennett and Srinivasam, 1983). The numbers of each species are presented as relative abundances.

To estimate SST, the Modern Analogue Technique (MAT) was performed with the software Paleoanalogs 3.0 and a predominantly South Atlantic database composed of a compilation of CLIMAP and MARGO core-top datasets ( $n = 468$ ). Each sample was compared with the ten best analogs in the modern database to reconstruct the annual, summer and winter SSTs. The best analogs were located between 5°N and 5°S, with an annual average SST of approximately 27 °C. The Square Chord function was used as the distance measure, and the relation between the observed SSTs and the reconstructed SSTs showed a correlation of  $R^2 = 0.9807$  ( $P > 95\%$ ). The average standard deviation was 0.8 °C, 0.6 °C and 1.2 °C for annual, summer and winter SST, respectively.

Finally, to reconstruct the SSS ( $\delta^{18}\text{O}_{\text{ivc-sw}}$ ), the summer SST and the  $\delta^{18}\text{O}_c$  were used to calculate the  $\delta^{18}\text{O}$  of the sea water ( $\delta^{18}\text{O}_{\text{sw}}$ ) using the equation proposed by Mulitza et al. (2003) for *G. ruber*. The values were corrected for ice volume (Waelbroeck et al., 2002). Then, the  $\delta^{18}\text{O}_{\text{sw}}$  was compared to the regional SSS– $\delta^{18}\text{O}_{\text{sw}}$  relationship presented by Weldeab et al. (2006). The error in SSS reconstruction accounts for the average standard deviation of summer SST (0.6 °C), which corresponds to 0.132‰, and the analytical error in oxygen isotope analyses (0.04‰), resulting in a cumulative error estimate of  $\delta^{18}\text{O}_{\text{sw}} \pm 0.17\%$ .

**Fig. 2.** Linear age–depth model for core MC 10/3 based on  $^{14}\text{C}$  AMS radiocarbon dating.

## 4. Results

### 4.1. Planktonic foraminiferal assemblage, SST and SSS

The planktonic foraminiferal assemblages were characterized by means of 26 taxonomic variables (species or morphotypes), as described in the CLIMAP and MARGO databases. Among all the observed species, eight were notably important for the paleoceanographic interpretation (Fig. 3). The dominant species were as follows: the surface dwellers *G. ruber* (white and pink) (55–70%), *Globigerinoides sacculifer* (with and without the final saclike chamber) (10–30%) and *Globigerinella siphonifera* (1–5%) (Fig. 3); the productivity/thermocline dwellers *Globigerina glutinata* (1–12%), *Neogloboquadrina dutertrei* (0–4%) and *Globorotalia menardii* (0–4%) (Fig. 3); and the deep dwellers *Globorotalia truncatulinoides* (left- and right-coiling) (0–4%) and *Globorotalia inflata* (0–0.6%) (Fig. 3), whose relative abundance did not exceed 1%.

The productivity/thermocline dwellers showed higher percentages prior to 21 cal kyr BP. Following this period, a strong reduction in abundances was observed for *G. glutinata* and *G. inflata*, the latter of which disappeared totally after 16 cal kyr BP (Fig. 3). The species *N. dutertrei* and *G. truncatulinoides* both presented highly variable percentages until 30 cal kyr BP. However, an overall smoothly decreasing trend in the record was noted for both species. The species *G. menardii* was extremely rare prior to 21 cal kyr BP but its occurrence rose abruptly after 17.5 cal kyr BP. Otherwise, the warm surface dwellers, mainly *G. siphonifera*, show a smooth increasing trend toward the present after 30 cal kyr BP (Fig. 3).

All SSTs calculated by MAT showed a decreasing trend between 40 and 30 cal kyr BP, followed by a slight increasing trend, mainly after 21 cal kyr BP, toward the present. The average values for winter, annual and summer temperatures were 25.3 °C, 26.6 °C and 26.9 °C, respectively (Fig. 4A, B and C). The SST range was higher for winter values ( $\sim 2$  °C) and lower for annual and summer values ( $\sim 1$  °C). However, the winter SST also exhibited the highest average standard deviation of approximately 1.2 °C. The average standard deviations for annual and summer SSTs were 0.8 °C and 0.6 °C, respectively, and for this factor, the annual and summer temperatures were very close to each other. The variation in seasonality was calculated by using the difference between summer and winter SSTs ( $\Delta\text{SST}$ ) (Fig. 4E). The  $\Delta\text{SST}$  range was approximately 2 °C, and higher values were found prior to 30 cal kyr BP. After that time, the  $\Delta\text{SST}$  values became smaller towards the top of the core.

The SSS remained relatively stable, with values between 36.8 and 37.6, until 21 cal kyr BP, when, at the onset of deglaciation, a strong decrease was observed, reaching the lowest value of 34.7 at 17.5 cal kyr BP (Fig. 5B). Following this excursion, the SSS increased back to values similar to those recorded prior to 21 cal kyr BP (Fig. 5B).

### 4.2. Oxygen stable isotope values

The  $\delta^{18}\text{O}_c$  values of the planktonic foraminifera *G. ruber* (white) were relatively high until 21 cal kyr BP, reaching a maximum of  $-0.35\%$  at approximately 22.8 cal kyr BP (Fig. 5A). After 21 cal kyr BP,

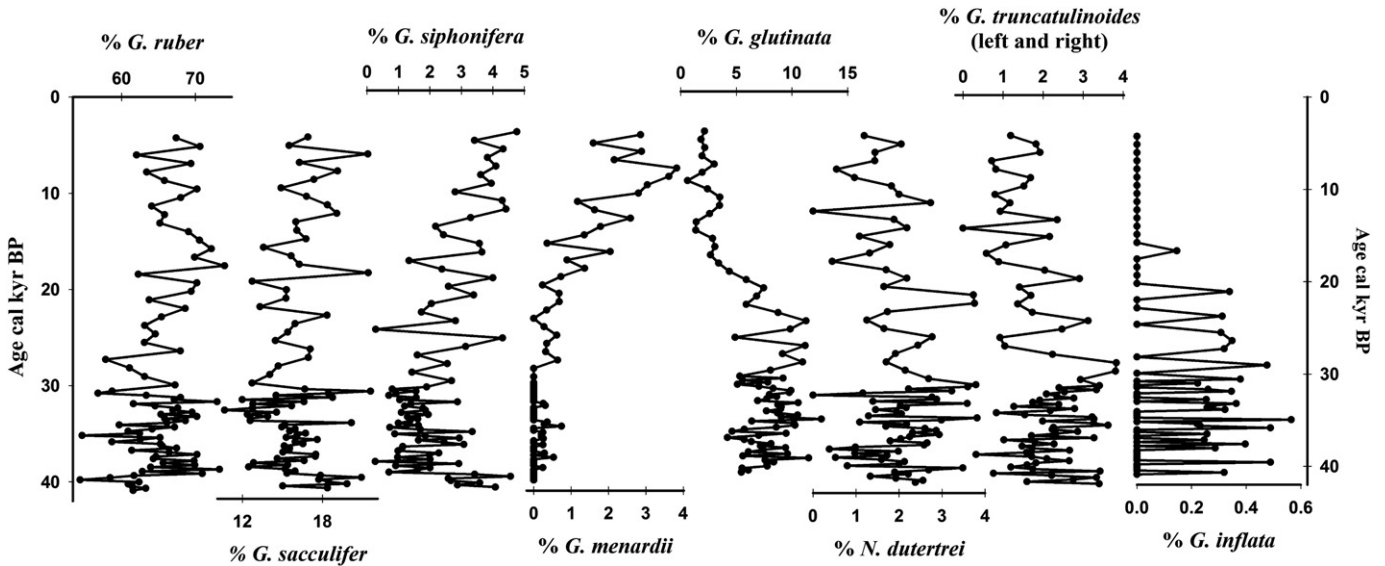


Fig. 3. Relative abundances (%) of the main species of planktonic foraminifera in the core MC 10/3.

a strong shift in the  $\delta^{18}O_c$ , approximately 1.2‰, marked the boundary between the deglaciation and the Holocene. The values reached a minimum of  $-1.8\text{‰}$  at approximately 10 cal kyr BP. The difference between the LGM and the Holocene was 1.46‰ (Fig. 5A).

5. Discussion

5.1. SST and SSS changes inferred from MAT and oxygen stable isotopes

The analysis of the oxygen isotopes from *G. ruber* showed two distinct patterns of change in the western equatorial Atlantic. These patterns are defined by a sharp decrease, approximately 1‰, in  $\delta^{18}O_c$  values after 21 cal kyr BP, which could have corresponded to a temperature increase of almost 4 °C. However, the SST calculated by MAT suggests an increase of approximately 1 °C. Therefore, the shift in oxygen isotopes cannot be solely attributed to temperature and must have a salinity component within its variation (Fig. 5).

Despite the salinity influence on oxygen isotopes, it is possible to assume that the western equatorial Atlantic experienced important SST warming after 30 cal kyr BP (Figs. 4 and 5). One portion of the SST rise can be attributed to external forcing, e.g., changes in seasonal insolation distribution across the tropical latitudes (Fig. 4D and E). Summer insolation increased smoothly over the last 40 cal kyr BP, which could have warmed the ocean surface. Calculation of the annual and summer  $SST_{MAT}$  produced virtually the same values, with only a 0.2 °C difference in the average standard deviation between them. It can therefore be concluded that summer SST has a greater influence on the annual trend than winter SST. Therefore, changes in summer SST forcing mechanisms can deeply affect the annual SST in the region and, consequently, circulation patterns.

Recently, a physical mechanism proposed by He et al. (2013) also showed that much of the early deglacial warming of the Southern Hemisphere was driven initially by changes in Northern Hemisphere orbital forcing and subsequently by increasing of atmospheric greenhouse gases. A Pacific LGM reconstruction hypothesized that the cause of tropical warming during deglaciation does not lie within the tropics but is related to insolation changes over the Southern Ocean that influenced the retreat of sea ice (Stott et al., 2007). This mechanism promoted enhanced ventilation of deep sea and a subsequent rise in atmospheric  $CO_2$ , which progressively acted rising the SST in mid and low Pacific latitudes. Such process also could be thought as a driver of the equatorial South Atlantic SST increase.

Moreover, during the period that covers the LGM and the deglaciation, the high latitudes of the northern hemisphere experienced extreme climatic fluctuations, i.e., Heinrich events and the sea-ice maximum that reduced northern SSTs by several degrees (Thornalley

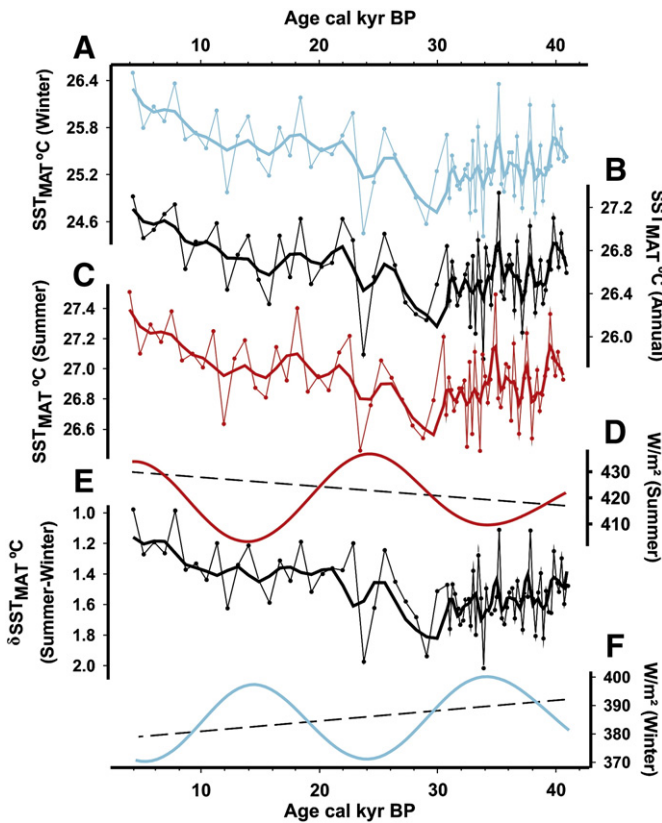


Fig. 4. A: Summer SST reconstructed by the MAT; B: Annual SST reconstructed by the MAT; C: Winter SST reconstructed by the MAT; D: Summer insolation at 4°S; E: Difference between summer and winter SST ( $\Delta SST$ ); F: Winter insolation at 4°S. The insolation data are available at <http://www.imcce.fr/Equipes/ASD/insola/earth/online/index.php>.

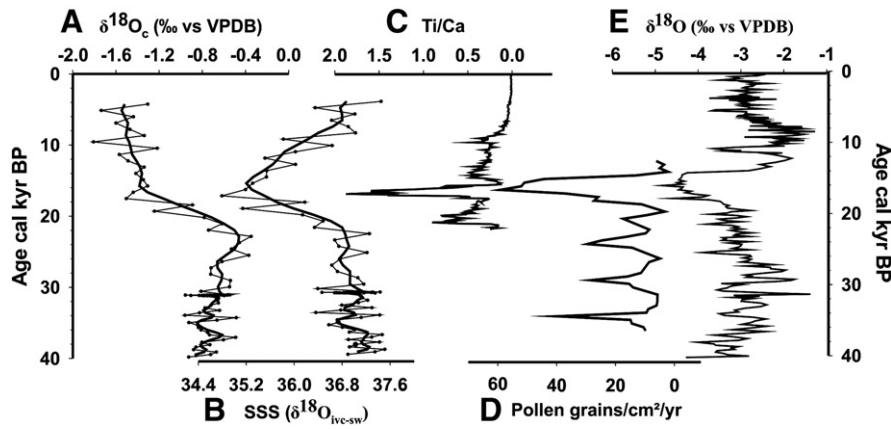


Fig. 5. A: Oxygen isotope composition of the species *G. ruber* for core MC 10/3. B: SSS reconstruction based on oxygen isotopes and summer SSTs for core MC 10/3. C: Ti/Ca ratios for core GeoB3104 (Arz et al., 1999). D: Pollen grains/cm<sup>2</sup>/yr from core GeoB3104-1 (Behling et al., 2000). E: Stable oxygen isotope profile for stalagmite BT2 (Cruz et al., 2005).

et al., 2011). However, as other reconstruction is proposed (Rühlemann et al., 1999; Vink et al., 2001; Lea et al., 2003), our findings indicated a lower variation in SST across the LGM and deglacial period. One possible explanation for this inter-hemispheric antiphasing is the ocean meridional circulation variability on a millennial time-scale (Knorr and Lohmann, 2003). The asynchronous relationship between the northern and southern latitudes has led to the concept of a bipolar seesaw that redistributes heat within the Atlantic Ocean (Stocker and Johnsen, 2003). Thus, the meltwater input into the North Atlantic, mainly during the deglacial period, strongly diminished the AMOC and the northward heat transport.

Numerical modeling has shown that a substantially weakened meridional circulation leads to significant and persistent remote responses outside the Atlantic that include the following: a southward shift of the ITCZ; weakened Walker circulation in the southern tropical Pacific; and weakened Indian and East Asian summer monsoons (Zhang and Delworth, 2005). Evidence from the LGM and deglaciation has shown significant changes in the position of the ITCZ that were concomitant with climate changes in the North Atlantic (Chiang et al., 2003). A rapid southward shift in the atmospheric ITCZ could account for the synchronicity in the tropical temperature and high-latitude changes during the LGM and deglacial (Lea et al., 2003). Additionally, the resulting hemisphere-wide adjustments in the atmospheric circulation due to southward ITCZ displacement strongly modified the surface currents in the western tropical Atlantic, causing a curtailment of the cross-tropical transport and strengthening the NBC retroflexion and the NECC (Wilson et al., 2011).

Such oscillations of the ITCZ also induce changes in the precipitation regimes that characterize many northern and southern tropical regions throughout the world. The wet periods of northeastern Brazil that enabled floristic exchanges between the Atlantic rainforest and the Amazonian rain forest are related to the cold intervals in Greenland (Behling et al., 2000; Wang et al., 2004). The southward displacement of the ITCZ and its belt of convective activity, mainly during Heinrich event 1, increased the erosion and transport of material from the continent into the ocean, as evidenced by the Ti/Ca and pollen grain flux data of surrounding areas (Fig. 5C and D) (Arz et al., 1999; Behling et al., 2000). ITCZ displacement was also associated with strong precipitation over the area and a two-unit reduction in the salinity between 21 and 17.5 cal kyr BP (Fig. 5) and most likely influenced the oxygen isotope values of *G. ruber*. The moisture over the study area, together with the convective activity over the Amazon basin, was also transported to southern Brazil via the South America monsoon system and generated a wet period synchronous with the low salinity signal (Cruz et al., 2005) (Fig. 5E).

Weldeab et al. (2006) argued that the changes in the western equatorial Atlantic during the Bøling-Allerød and Younger Dryas were synchronous with the warming of the southern high latitudes, implying that the sea surface conditions over the tropical region were amplified by southern Atlantic warming, as well as by the associated heat and salinity supply via the SEC. Our data indicate that the supply of warmth and salt via SEC after 17.5 cal kyr BP may also be related to the reactivation of Agulhas leakage during the deglaciation, as will be discussed in the next Section.

## 5.2. Planktonic foraminifera as tracers for water column properties

Planktonic foraminiferal assemblages vary in response to the hydrographic properties of the water column (Schiebel and Hemleben, 2000). In the western equatorial Atlantic, two different conditions of the water column existed, as suggested by fluctuations in the foraminiferal assemblage that followed the main shift in  $\delta^{18}\text{O}_c$  and SSS after 21 cal kyr BP.

Between the core bottom and 21 cal kyr BP, *G. glutinata* was present at higher abundances than during later periods. The species *N. dutertrei* and *G. truncatulinoides* had smooth increasing trends, and even *G. inflata*, which was rare in most of the record, was present during this period (Fig. 3). At northern high latitudes, *G. glutinata* often has maximum abundances in response to phytoplankton development during the spring and lives near the thermocline, no deeper than 130–150 m (Schiebel and Hemleben, 2000; Schmuker and Schiebel, 2002; Kuroyanagi and Kawahata, 2004; Lončarić et al., 2006). Based on these modern ecological preferences, we assume that higher abundances of *G. glutinata* prior to 21 cal kyr BP (Fig. 3) are a response to a water column that was more homogeneous, less oligotrophic, and relatively colder than the following periods.

The conditions inferred from the planktonic foraminiferal assemblage prior to 21 cal kyr BP could be the result of a weaker SEC, which consequently reduced the upper transport of warm waters toward the South American coast. The southerly position of the ITCZ during the glacial period also contributed to the development of this scenario. According to Rodrigues et al. (2007), a southerly displacement of the ITCZ shifts the SEC bifurcation to its northernmost position, which increases the BC and reduces the NBC flux. The weaker extra-tropical heat exchange due to reduced NBC favors productive/deep-dwelling species and supports a glacial climate.

In the second portion of the record, with the shift in  $\delta^{18}\text{O}_c$  corresponding to the onset of deglaciation, SSS and SSTs indicate a transition to warmer and more oligotrophic conditions in the region that was coupled with a strong reduction in the species related to thermocline/

productivity and deep water, especially *G. glutinata* and *G. inflata* (Fig. 3). From 21 cal kyr BP to the present, the abundances of the surface-dwelling species *G. ruber*, *G. sacculifer* and especially *G. siphonifera* (Ravelo et al., 1990) increased in the record.

The change in the faunal assemblage following 21 cal kyr BP may be linked to both the SST increase and the SSS decrease of two units (Fig. 5). These changes supported the surface-dwelling species but established more stratified conditions within the water column and reduced the depth of the thermocline. Climatological studies have shown that intense precipitation associated with the ITCZ in the tropical Atlantic can produce fresher, less dense shallow waters, generating “barrier layers” that profoundly affect the water column structure (Ferry and Riverdin, 2004; Mignot et al., 2007; Da-Allada et al., 2013).

Furthermore, the reappearance of the species *G. menardii*, which is often employed as an interglacial/glacial indicator, was recorded in core MC 10/3 before its reappearance on the southern Brazilian margin (Cremer et al., 2007). The reappearance of *G. menardii* at the study site was constrained to approximately 17.5 cal kyr BP and was roughly concordant with the SSS recovery after the two-unit fall between 21 and 17.5 cal kyr BP (Fig. 5). The only source for re-seeding *G. menardii* into the Atlantic after the LGM is around the Cape of Good Hope (Knorr and Lohmann, 2003). Hence, the reestablishment of Agulhas leakage may have contributed to the resumption of the AMOC and may have affected the western equatorial Atlantic by introducing warm, salty waters into the SEC, especially after 17.5 cal kyr BP. Such conditions were demonstrated in a modeling study by Biastoch and Böning (2013). Their model suggests that changes in southern hemisphere winds produce a rapid dynamic adjustment in Agulhas leakage, resulting in the potential salinification and densification of upper thermocline waters of the South Atlantic. Additionally, the reduction in seasonality differences between summer and winter (Fig. 4E) could contribute to the transition to near-modern NBC circulation and inter-hemispheric heat exchange at the end of deglaciation.

## 6. Conclusions

The sediment record of core MC 10/3, collected from the northeast Brazil margin, allowed the reconstruction of paleoceanographic conditions over the last 40 kyr. The oxygen isotope composition of the planktonic foraminifer *G. ruber* showed a strong shift (>1‰) after 21 cal kyr BP. SST changes cannot be totally responsible for such a large fluctuation because the SST indicated by MAT suggests only a slight warming of 1 °C after 30 cal kyr BP. However, the SSS reconstruction recorded a two-unit reduction between 21 and 17.5 cal kyr BP. This low salinity signal may be the result of a southward displacement of the ITCZ during cold events in the northern Atlantic, e.g., Heinrich event 1, which increased the precipitation over the region and influenced the carbonate isotopic signal.

The planktonic foraminiferal assemblages corroborate these interpretations. The species related to productive/thermocline and deep-water masses (*G. glutinata*, *N. dutertrei*, *G. truncatulinoides* and *G. inflata*) were more abundant prior to 21 cal kyr BP when the water column was colder and less stratified. After 21 cal kyr BP, lower salinity in surface waters strengthened the stratification and, in concert with a slight increase in SST, favored the surface-dwelling species (*G. ruber*, *G. sacculifer* and *G. siphonifera*) and reduced the abundance of productivity/thermocline- and deep-dwelling species. The species *G. menardii* was absent during most of the record, and its reappearance, mainly after 17.5 cal kyr BP, may signal the resumption of the Agulhas leakage because this is the only way to reintroduce this species into the Atlantic. The influence of warm, salty waters from Agulhas leakage on the SEC could be responsible for the increase in salinity after 17.5 cal kyr BP. Our results show that the western tropical Atlantic can respond to external and internal forcing mechanisms on millennial time-scales, such as insolation distribution related to seasonality changes (especially those linked to summer SST),

atmospheric adjustments and meridional Atlantic circulation variability triggered by northern and southern latitudes.

## Acknowledgments

We thank the European Science Foundation (ESF) and the members of project RETRO for coordinating the sediment sampling. We are grateful to Abdelfettah Sifeddine for providing helpful comments during the preparation and to Conselho Nacional de Desenvolvimento Científico e Tecnológico (CNPq) for the financial support. We are also especially grateful to the two reviewers for their valuable comments, which strengthened the manuscript.

## Appendix A. Supplementary data

Supplementary data associated with this article can be found in the online version, at <http://dx.doi.org/10.1016/j.palaeo.2014.01.001>. These data include Google map of the most important areas described in this article.

## References

- Angulo, R.J., Souza, M.C., Reimer, P., Sasaoka, S.K., 2005. Reservoir effect of the southern and southeastern Brazilian coast. *Radiocarbon* 47 (1), 67–73.
- Arz, H.W., Pätzold, J., Wefer, G., 1998. Correlated millennial-scale changes in surface hydrography and terrigenous sediment yield inferred from last-glacial marine deposits off northeastern Brazil. *Quat. Res.* 50, 157–166.
- Arz, H.W., Pätzold, J., Wefer, G., 1999. The deglacial history of the western tropical Atlantic as inferred from high resolution stable isotope records off northeastern Brazil. *Earth Planet. Sci. Lett.* 167, 105–117.
- Barker, S., Diz, P., Vautravers, M.J., Pike, J., Knorr, G., Hall, I.R., Broecker, W.S., 2009. Inter-hemispheric Atlantic seesaw response during the last deglaciation. *Nature* 457 (7233), 1097–1102. <http://dx.doi.org/10.1038/nature07770>.
- Bé, A.W.H., 1977. An ecological, zoogeographic and taxonomic review of recent planktonic foraminifera. In: Ramsay, A.T.S. (Ed.), *Oceanic Micropaleontology*. Academic Press, London, pp. 1–100.
- Beal, L.M., De Ruijter, W.P.M., Biastoch, A., Zahn, R., 2011. On the role of the Agulhas system in ocean circulation and climate. *Nature* 472 (7344), 429–436. <http://dx.doi.org/10.1038/nature09983>.
- Behling, H., Arz, H.W., Wefer, G., 2000. Late Quaternary vegetational and climate dynamics in northeastern Brazil, inferences from marine core GeoB 3104–1. *Quat. Sci. Rev.* 19, 981–994.
- Biastoch, A., Böning, C.W., 2013. Anthropogenic impact on Agulhas leakage. *Geophys. Res. Lett.* 40 (6), 1138–1143. <http://dx.doi.org/10.1002/grl.50243>.
- Biastoch, A., Böning, C.W., Lutjeharms, J.R.E., 2008. Agulhas leakage dynamics affects decadal variability in Atlantic overturning circulation. *Nature* 456 (7221), 489–492. <http://dx.doi.org/10.1038/nature07426>.
- Broecker, W.S., 1998. Paleocirculation during the last deglaciation: a bipolar seesaw? *Paleoceanography* 13 (2), 119–121.
- Chang, P., Ji, L., Li, H., 1997. A decadal climate variation in the tropical Atlantic Ocean from thermodynamic air–sea interactions. *Nature* 385, 516–518.
- Chiang, J.C.H., Biasutti, M., Battisti, D.S., 2003. Sensitivity of the Atlantic Intertropical Convergence Zone to Last Glacial Maximum boundary conditions. *Paleoceanography* 18 (4), 1–18. <http://dx.doi.org/10.1029/2003PA000916>.
- Cremer, M., Gonthier, E., Duprat, J., Faugères, J., Courp, T., 2007. Late Quaternary variability of the sedimentary record in the Sao Tome deep-sea system (South Brazilian basin). *Mar. Geol.* 236, 223–245. <http://dx.doi.org/10.1016/j.margeo.2006.10.032>.
- Cruz, C., Burns, S.J., Karmann, I., 2005. Insolation-driven changes in atmospheric circulation over the past 116,000 years in subtropical Brazil. *Nat. Geosci.* 63–66. <http://dx.doi.org/10.1029/2003JB002684>.
- Da-Allada, C.Y., Alory, G., Penhoat, Y., Kestenare, E., Durand, F., Hounkonnou, N.M., 2013. Seasonal mixed-layer salinity balance in the tropical Atlantic Ocean: mean state and seasonal cycle. *J. Geophys. Res.* 118, 332–345. <http://dx.doi.org/10.1029/2012JC008357>.
- Ferry, N., Riverdin, G., 2004. Sea surface salinity interannual variability in the western tropical Atlantic: an ocean general circulation model study. *J. Geophys. Res.* 109 (C5), C05026. <http://dx.doi.org/10.1029/2003JC002122>.
- Fonseca, C.A., Goni, G.J., Johns, W.E., Campos, E.J.D., 2004. Investigation of the North Brazil Current retroflection and North Equatorial Countercurrent variability. *Geophys. Res. Lett.* 31 (21), 1–5. <http://dx.doi.org/10.1029/2004GL020054>.
- Goelzer, H., Mignot, J., Levermann, A., Rahmstorf, S., 2006. Tropical versus high latitude freshwater influence on the Atlantic circulation. *Clim. Dyn.* 27 (7–8), 715–725. <http://dx.doi.org/10.1007/s00382-006-0161-5>.
- Goni, G.J., Johns, W.E., 2001. A census of North Brazil Current Rings observed from TOPEX/POSEIDON altimetry: 1992–1998. *Geophys. Res. Lett.* 28 (1), 1–4.
- Guihou, A., Pichat, S., Govin, A., Nave, S., Michel, E., Duplessy, J.-C., Telouk, P., Labeyrie, L., 2011. Enhanced Atlantic Meridional Overturning Circulation supports the Last Glacial Inception. *Quat. Sci. Rev.* 30 (13–14), 1576–1582. <http://dx.doi.org/10.1016/j.quascirev.2011.03.017>.

- Haarsma, R.J., Campos, E.J.D., Drijfhout, S., Hazeleger, W., Severijns, C., 2011. Impacts of interruption of the Agulhas leakage on the tropical Atlantic in coupled ocean–atmosphere simulations. *Clim. Dyn.* 36 (5–6), 989–1003. <http://dx.doi.org/10.1007/s00382-009-0692-7>.
- He, F., Shakun, J.D., Clark, P.U., Carlson, A.E., Liu, Z., Otto-Bliesner, B.L., Kutzbach, J.E., 2013. Northern Hemisphere forcing of Southern Hemisphere climate during the last deglaciation. *Nature* 494 (7435), 81–85. <http://dx.doi.org/10.1038/nature11822>.
- Johns, W., Lee, T., Beardsley, R.C., Candela, J., Limeburner, R., Castro, B., 1998. Annual cycle and variability of the North Brazil Current. *J. Phys. Oceanogr.* 103–128. [http://dx.doi.org/10.1175/15200485\(1998\)028%3C0103:ACAVAC%3E2.0.CO;3B2](http://dx.doi.org/10.1175/15200485(1998)028%3C0103:ACAVAC%3E2.0.CO;3B2).
- Kennett, J.P., Srinivasam, M.S., 1983. *Neogene Planktonic Foraminifera: a Phylogenetic Atlas*. Hutchinson Ross Publishing Company, Stroudsburg 273.
- Knorr, G., Lohmann, G., 2003. Southern Ocean origin for the resumption of Atlantic thermohaline circulation during deglaciation. *Nature* 424. <http://dx.doi.org/10.1038/nature01855>.
- Kuroyanagi, A., Kawahata, H., 2004. Vertical distribution of living planktonic foraminifera in the seas around Japan. *Mar. Micropaleontol.* 53 (1–2), 173–196. <http://dx.doi.org/10.1016/j.marmicro.2004.06.001>.
- Lea, D.W., Pak, D.K., Peterson, L.C., Hughen, K.A., 2003. Synchronicity of tropical and high-latitude Atlantic temperatures over the Last Glacial termination. *Science* 301, 1361–1364.
- Lončarić, N., Peeters, F.J.C., Kroon, D., Brummer, G.J.A., 2006. Oxygen isotope ecology of recent planktonic foraminifera at the central Walvis Ridge (SE Atlantic). *Paleoceanography* 21. <http://dx.doi.org/10.1029/2005PA001207>.
- Lux, M., Mercier, H., Arhan, M., 2001. Interhemispheric exchanges of mass and heat in the Atlantic Ocean in January–March 1993. *Deep-Sea Res.* 1 48, 605–638.
- Marino, G., Zahn, R., Ziegler, M., Purcell, C., Knorr, G., Hall, I.R., Ziveri, P., et al., 2013. Agulhas salt-leakage oscillations during abrupt climate changes of the Late Pleistocene. *Paleoceanography* 28. <http://dx.doi.org/10.1002/palo.20038>.
- Mignot, J., de Boyer Montégut, C., Lazar, A., Cravatte, S., 2007. Control of salinity on the mixed layer depth in the world ocean: 2. Tropical areas. *J. Geophys. Res.* 112 (C10), C10010. <http://dx.doi.org/10.1029/2006JC003954>.
- Mulitza, S., Boltovskoy, D., Donner, B., Meggers, H., Paul, A., Wefer, G., 2003. Temperature:  $\delta^{18}\text{O}$  relationships of planktonic foraminifera collected from surface waters. *Palaeogeogr. Palaeoclimatol. Palaeoecol.* 202 (1–2), 143–152. [http://dx.doi.org/10.1016/S0031-0182\(03\)00633-3](http://dx.doi.org/10.1016/S0031-0182(03)00633-3).
- Niebler, H.S., Mulitza, S., Donner, B., Arz, H., Patzold, J., Wefer, G., 2003. Sea-surface temperatures in the equatorial and South Atlantic Ocean during the Last Glacial Maximum (23–19 ka). *Paleoceanography* 18. <http://dx.doi.org/10.1029/2003PA000902>.
- Parker, F.L., 1962. Planktonic foraminiferal species in Pacific sediments. *Micropaleontology* 8 (2), 219–254.
- Peterson, L., Haug, G., 2006. Variability in the mean latitude of the Atlantic Intertropical Convergence Zone as recorded by riverine input of sediments to the Cariaco Basin (Venezuela). *Palaeogeogr. Palaeoclimatol. Palaeoecol.* 234 (1), 97–113. <http://dx.doi.org/10.1016/j.palaeo.2005.10.021>.
- Pflaumann, U., Sarnthein, M., Chapman, M., Duprat, J., Huels, M., Kiefer, T., Maslin, M., Schulz, H., van Kreveld, S., Vogelsang, E., Weinelt, M., 2003. North Atlantic: sea-surface conditions reconstructed by GLAMAP-2000. *Paleoceanography* 18. <http://dx.doi.org/10.1029/2002PA000774>.
- Ravelo, A.C., Fairbanks, R.G., Philander, S.G.H., 1990. Reconstructing tropical Atlantic hydrography using planktonic foraminifera and an ocean model. *Paleoceanography* 5 (3), 409–431.
- Rodrigues, R.R., Rothstein, L.M., Wimbush, M., 2007. Seasonal Variability of the South Equatorial Current Bifurcation in the Atlantic Ocean: A Numerical Study. *Journal of Physical Oceanography* 37. <http://dx.doi.org/10.1175/JPO2983.1>.
- Rühlemann, C., Mulitza, S., Müller, P.J., Wefer, G., Zahn, R., 1999. Warming of the tropical Atlantic Ocean and slowdown of thermohaline circulation during the last deglaciation. *Nature* 402, 511–514.
- Schiebel, R., Hemleben, C., 2000. Interannual variability of planktonic foraminiferal populations and test flux in the eastern North Atlantic Ocean (JGOFS). *Deep-Sea Res.* II 47, 1809–1852.
- Schmuker, B., Schiebel, R., 2002. Planktonic foraminifera and hydrography of the eastern and northern Caribbean Sea. *Mar. Micropaleontol.* 46 (3–4), 387–403. [http://dx.doi.org/10.1016/S0377-8398\(02\)00082-8](http://dx.doi.org/10.1016/S0377-8398(02)00082-8).
- Schott, A.F., Stramma, L., Fischer, J., 1995. The warm water inflow into the western tropical Atlantic boundary regime, spring 1994. *J. Geophys. Res.* 100 (12), 745–760. <http://dx.doi.org/10.1029/95JC02803>.
- Servain, J., Busalacchi, A.J., McPhaden, M.J., Moura, A.D., Reverdin, G., Vianna, M., Zebiak, S.E., 1998. A Pilot Research Moored Array in the Tropical Atlantic (PIRATA). *Bull. Am. Meteorol. Soc.* 79 (10), 2019–2031.
- Stocker, T.F., Johnsen, S.J., 2003. A minimum thermodynamic model for the bipolar seesaw. *Paleoceanography* 18 (4). <http://dx.doi.org/10.1029/2003PA000920>.
- Stott, L., Timmermann, A., Thunell, R., 2007. Southern Hemisphere and deep-sea warming led deglacial atmospheric CO<sub>2</sub> rise and tropical warming. *Science* 318 (5849), 435–438. <http://dx.doi.org/10.1126/science.1143791>.
- Stramma, L., Schott, F., 1999. The mean flow field of the tropical Atlantic Ocean. *Atlantic Deep-Sea Res.* II 46, 279–303.
- Stuiver, M., Reimer, P.J., Bard, E., Beck, J.W., Burr, G.S., Hughen, K.A., Kromer, B., McCormac, F.G., von der Plicht, J., Spurk, M., 1998. INTCAL98 radiocarbon age calibration, 24,000–0 cal B.P. *Radiocarbon* 40, 1041–1083.
- Thornalley, D.J.R., Elderfield, H., McCave, I.N., 2011. Reconstructing North Atlantic deglacial surface hydrography and its link to the Atlantic overturning circulation. *Glob. Planet. Chang.* 79 (3–4), 163–175. <http://dx.doi.org/10.1016/j.gloplacha.2010.06.003>.
- Vink, A., Rühlemann, C., Zonneveld, K.A.F., Mulitza, S., Hüls, M., Willems, H., 2001. Shifts in the position of the North Equatorial Current and rapid productivity changes in the western Tropical Atlantic during the last glacial. *Paleoceanography* 16, 479–490.
- Waelbroeck, C., Labeyrie, L., Michel, E., Duplessy, J.C., McManus, J.F., Lambeck, K., Balbon, E., et al., 2002. Sea-level and deep water temperature changes derived from benthic foraminifera isotopic records. *Quat. Sci. Rev.* 21 (1–3), 295–305. [http://dx.doi.org/10.1016/S0277-3791\(01\)00101-9](http://dx.doi.org/10.1016/S0277-3791(01)00101-9).
- Wang, X., Auler, A.S., Edwards, R.L., Cheng, H., Cristalli, P.S., Smart, P.L., Richards, D.A., Shen, C.C., 2004. Wet periods in northeastern Brazil over the past 210 kyr linked to distant climate anomalies. *Nature* 432 (7018), 740–743. <http://dx.doi.org/10.1038/nature03067>.
- Weldeab, S., Schneider, R.R., Kölling, M., 2006. Deglacial sea surface temperature and salinity increase in the western tropical Atlantic in synchrony with high latitude climate instabilities. *Earth Planet. Sci. Lett.* 241 (3–4), 699–706. <http://dx.doi.org/10.1016/j.epsl.2005.11.012>.
- Wilson, K.E., Maslin, M.A., Burns, S.J., 2011. Evidence for a prolonged retroflexion of the North Brazil Current during glacial stages. *Palaeogeogr. Palaeoclimatol. Palaeoecol.* 301 (1–4), 86–96. <http://dx.doi.org/10.1016/j.palaeo.2011.01.003>.
- Zhang, R., Delworth, T.L., 2005. Simulated tropical response to a substantial weakening of the Atlantic. *J. Clim.* 18, 1853–1860.
- Zickfeld, K., Levermann, A., Morgan, M.G., Kuhlbrodt, T., Rahmstorf, S., Keith, D.W., 2007. Expert judgements on the response of the Atlantic meridional overturning circulation to climate change. *Clim. Chang.* 82 (3–4), 235–265. <http://dx.doi.org/10.1007/s10584-007-9246-3>.